

RESEARCH

Open Access



Alteration of the cortical morphology in classical trigeminal neuralgia: voxel-, deformation-, and surface-based analysis

Xiuhong Ge^{1,2†}, Luoyu Wang^{1,2†}, Lei Pan¹, Haiqi Ye¹, Xiaofen Zhu¹, Sandra Fan³, Qi Feng¹, Quan Du^{4*†}, Wenhua Yu^{4*†} and Zhongxiang Ding^{1,2*†} 

Abstract

Objective This study aimed to combine voxel-based morphometry, deformation-based morphometry, and surface-based morphometry to analyze gray matter volume and cortex shape in classical trigeminal neuralgia patients.

Methods This study included 79 classical trigeminal neuralgia patients and age- and sex-matched 81 healthy controls. The aforementioned three methods were used to analyze brain structure in classical trigeminal neuralgia patients. Spearman correlation analysis was used to analyze the correlation of brain structure with the trigeminal nerve and clinical parameters.

Results The bilateral trigeminal nerve was atrophied, and the ipsilateral trigeminal nerve volume was smaller than the contralateral volume in the classical trigeminal neuralgia. The gray matter volume of Temporal_Pole_Sup_R and Precentral_R was found to be decreased using voxel-based morphometry. The gray matter volume of Temporal_Pole_Sup_R had a positive correlation with disease duration and a negative correlation with the cross-section area of the compression point and the quality-of-life score in trigeminal neuralgia. The gray matter volume of Precentral_R was negatively correlated with the ipsilateral volume of the trigeminal nerve cisternal segment, cross-section area of compression point, and visual analogue scale. The gray matter volume of Temporal_Pole_Sup_L was found to be increased using deformation-based morphometry and had a negative correlation with the self-rating anxiety scale. The gyrification of the middle temporal gyrus_L increased and the Postcentral_L thickness decreased, as detected using surface-based morphometry.

[†]Xiuhong Ge and Luoyu Wang contributed equally to this work.

[†]Xiuhong Ge and Luoyu Wang are the co-first author.

[†]Quan Du, Wenhua Yu and Zhongxiang Ding contributed equally to this work as corresponding authors.

*Correspondence:

Quan Du
duquan76@zuaa.zju.edu.cn
Wenhua Yu
ywh699@126.com
Zhongxiang Ding
hangzhoudzx73@126.com

¹ Department of Radiology, Affiliated Hangzhou First People's Hospital, Zhejiang University School of Medicine, Hangzhou 310000, People's Republic of China

² Department of Radiology, Key Laboratory of Clinical Cancer Pharmacology and Toxicology Research of Zhejiang Province, Cancer Center, Affiliated Hangzhou First People's Hospital Zhejiang University School of Medicine Shangcheng District, No.261, Huansha Road Zhejiang Province, Hangzhou 310006, China

³ Zhejiang Chinese Medical University, Hangzhou, China

⁴ Department of Neurosurgery, Affiliated Hangzhou First People's Hospital, Zhejiang University School of Medicine, Hangzhou 310000, People's Republic of China



© The Author(s) 2023. **Open Access** This article is licensed under a Creative Commons Attribution 4.0 International License, which permits use, sharing, adaptation, distribution and reproduction in any medium or format, as long as you give appropriate credit to the original author(s) and the source, provide a link to the Creative Commons licence, and indicate if changes were made. The images or other third party material in this article are included in the article's Creative Commons licence, unless indicated otherwise in a credit line to the material. If material is not included in the article's Creative Commons licence and your intended use is not permitted by statutory regulation or exceeds the permitted use, you will need to obtain permission directly from the copyright holder. To view a copy of this licence, visit <http://creativecommons.org/licenses/by/4.0/>. The Creative Commons Public Domain Dedication waiver (<http://creativecommons.org/publicdomain/zero/1.0/>) applies to the data made available in this article, unless otherwise stated in a credit line to the data.

Conclusions The gray matter volume and cortical morphology of pain-related brain regions were correlated with clinical and trigeminal nerve parameters. voxel-based morphometry, deformation-based morphometry, and surface-based morphometry complemented each other in analyzing the brain structures of patients with classical trigeminal neuralgia and provided a basis for studying the pathophysiology of classical trigeminal neuralgia.

Highlights

- (1) We first applied the three methods (VBM, DBM, and SBM) to the brain structure study in CTN and found that the three methods were complementary.
- (2) Some of the different brain regions correlated with clinical parameters, TGNcV, and CSA of the compression point.

Keywords Classical trigeminal neuralgia, Cortex shape, Voxel-based morphometry, Deformation-based morphometry, Gray matter volume, Surface-based morphometry

Graphical Abstract

Ge X | The Journal of Headache and Pain
SPRINGER NATURE



1. Key Message

In classical trigeminal neuralgia patients: GMV and cortical morphology of pain-related brain regions correlate with clinical and trigeminal nerve parameters



2. Main Results

- *TGN in classical TN*: Bilateral atrophy, lower ipsilateral volume
- *GMV of TPSR and PR*: Decreased
- *GMV of TPSR*: Correlation with disease duration, negative correlation with compression point cross-section area and QoL. *GMV of PR*: Negative correlation with ipsilateral volume of TGN cisternal segment, compression point cross-section area, VAS
- *GMV of TPSL*: Increased. Negative correlation with self-rating anxiety scale
- Gyrfication of middle temporal gyrus_L: Increased and PL thickness decreased

3. Methods

Study type: Clinical study

Study aim: To analyze the gray matter volume and cortex shape in classical TN patients based on structural MRI

Study cohort: 79 classical TN patients, 81 age-/ sex-matched healthy controls

Methods: Combined the voxel-based morphometry, deformation-based morphometry, and surface-based morphometry to analyze the brain structure difference between TN patients and healthy controls. Spearman correlation analysis to analyze correlation of brain structure with TGN and clinical parameters

Sample size



160

Abbreviations: Trigeminal neuralgia (TN), trigeminal nerve (TGN), quality-of-life (QoL), visual analogue scale (VAS), gray matter volume (GMV), Temporal_Pole_Sup_R (TPSR), Temporal_Pole_Sup_L (TPSL), Precentral_R (PR), Precentral_L (PL)

Creative Commons License BY-ND 4.0

Introduction

Classical trigeminal neuralgia (CTN) is a chronic neurogenic pain distributed in the trigeminal sensory area [1–3], characterized by sudden, transient, electric shock-like pain [4]. Most patients present with purely paroxysmal pain, whereas some of them present with concomitant continuous pain [5, 6] which up to 49 percent [7, 8]. The pain is often triggered by the harmless actions in daily life (washing face, eating, brushing

teeth, etc.) and is called the worst pain that human beings can endure [4].

According to the third edition of the International Classification of Headache Disorders (ICHD-3), CTN develops without any apparent cause other than neurovascular compression (NVC), which producing major morphological changes on the trigeminal nerve root [6, 9, 10]. NVC can cause demyelination of the nerve near the compression point, resulting in a short circuit

between the fibers involved in pain production and those mediating light touch, causing the pain [11]. NVC can cause a reduction in trigeminal nerve (TGN) volume. A study of the postoperative histopathological parameters showed axon atrophy and demyelination of the TGN in patients with trigeminal neuralgia (TN) [12]. The imaging also showed that the ipsilateral TGN atrophy [1, 13–15] and the cross-sectional area (CSA) of the compression point were smaller [16] in patients with CTN compared with healthy controls (HCs).

A certain correlation existed between the TGN morphology and the changing brain structure of patients with CTN [17, 18]. Many recent studies showed that the brain structure changed in patients with CTN, which included the gray matter volume (GMV) [2, 12, 16, 19–27] and cortical morphology. The brain regions in which the GMV changed were mainly the frontal lobe, temporal lobe, parietal lobe, thalamus, hippocampus, and cerebellum; the GMV changed differently in different studies. The changes in cortical morphology mainly included the cortical thickness [19, 26, 28–32], local gyrification index (LGI) [28, 30], sulcal depth [30], surface area, and myelin level [31].

Voxel-based morphometry (VBM) compares the local GMV at the voxel level, converting brain images into standard space to compensate the global differences and preserve the local differences in the distribution of gray matter (GM) cortex [33, 34]. Deformation-based morphometry (DBM) characterizes the differences in the vector fields, which describe global differences in the brain shape [35]. The two methods provide a comprehensive assessment of anatomical differences throughout the brain cortex [36, 37]. DBM is more sensitive to the atrophy of subcortical areas [38, 39] and the anatomical information exists in the deformation field [40]. Some studies suggested that DBM could replace VBM [41]. Other studies also found that the brain regions detected by the two methods were similar; only the clusters were different [42].

Surface-based morphometry (SBM) matches the gyration and groove geometry to the spherical map of the expansion, which greatly reduces the potential misalignment caused by complex folding patterns and the change in global volume [43]. Different from VBM and DBM that analyze the GMV, SBM is used to examine different characteristics of the cortex, for example, cortical thickness, sulcal depth, surface area, gyrification, and so on [43]. The aforementioned three methods provided the measurement of the brain structure, not redundant information [43, 44]. They revealed different aspects of the brain structure, implying that combined the three methods may further contribution to the study of neurogenic diseases. The combination of the three methods focuses on

the Parkinson's disease [42, 45], musical training [46], and chronic stroke [47], but has not been applied to CTN.

In this study, we combined VBM, DBM, and SBM to analyze the brain structure in patients with CTN. Our hypotheses were as follows. First, the GMV and cortical morphology of the pain-related brain regions in patients with CTN changed. Second, some of the changes in the brain included corrections in clinical parameters, such as visual analogue scale (VAS) scores, disease duration, and so on. Finally, the VBM, DBM, and SBM methods complemented each other in analyzing the brain structure of patients with CTN and providing a basis for studying CTN pathophysiology.

Materials and methods

The local ethics committee of the Affiliated Hangzhou First People's Hospital, Zhejiang University School of Medicine approved this prospective study (IRB# No. 202107002). The study was carried out following the Declaration of Helsinki. All the participants provided written informed consent.

Participants

A total of 88 patients with CTN and 85 age- and sex-matched HCs were recruited from the Affiliated Hangzhou First People's Hospital, Zhejiang University School of Medicine. The inclusion criteria for patients with CTN were as follows: (1) patients diagnosed with CTN according to ICHD-3 [6], which is that the CTN developing without apparent cause other than neurovascular compression [demonstration on MRI or during surgery of neurovascular compression (not simply contact), with morphological changes in the trigeminal nerve root]; (2) unilateral pain in the distribution of one or more branches of the TGN; (3) conventional magnetic resonance imaging (MRI) T1WI and T2WI sequence examinations revealing no evident abnormal brain signals; (4) no additional neurological or sensory deficits in all patients; (5) no previous surgical or other invasive procedures for CTN; (6) no contraindications to MRI; (7) aged 20–70 years; and (8) right-handedness. The exclusion criteria were as follows: (1) patients with CTN undergoing surgical treatment; (2) headaches, or other paroxysmal or chronic pain conditions; (3) a family history of headache or other types of pain in first-degree relatives; (4) other somatic or psychiatric conditions; and (5) contraindications to MRI. The inclusion criteria for the HCs were as follows: (1) age between 20 and 70 years; (2) good physical condition, with no history of tumors and mental diseases; (3) right-handedness; and (4) consent to join the study. The exclusion criteria were as follows: (1) headache or other chronic pain diseases; (2) MRI for

contraindications, such as claustrophobia; and (3) severe hypertension, diabetes, and other diseases affecting brain function.

Neuropsychological assessments

The psychiatrist evaluated the clinical psychological status of all participants. The quality-of-life score of patients with TN (TN QOLS) was used to assess the quality of life, including four dimensions: symptoms, physical function field, psychology (or emotion) field, and society (including family relationships) [48]. The mini-mental state examination (MMSE), the self-rating depression scale (SDS), and the self-rating anxiety scale (SAS) were used to evaluate cognitive function, depression, and anxiety symptoms.

Pain evaluation

The VAS was used to assess the intensity of trigeminal neuralgia in patients with CTN in the last week. The researchers guided patients with CTN in rating their pain on a scale of 0–10 using a 10-cm ruler, with the higher score indicating greater pain intensity. A score of “0” represented no pain, and a score of “10” meant intolerable pain.

MRI acquisition and analysis

All participants underwent MRI using a 3.0 T MRI scanner (Siemens, MAGNETOM Verio, Germany) and an eight-channel phased-array head coil. The 3D damage-gradient echo sequences were used to collect functional data. The parameters were as follows: 176 *structural images*, *repetition time (TR) = 1900 msec*, *echo time (TE) = 2.52 msec*, *thickness = 1 mm*, *field of view (FOV) = 256 × 256 mm²*, Trigeminal 3D volume interpolation body part examination (3D-VIBE) data were acquired using the following parameters: *TR = 10 ms*, *TE = 3.69 ms*, *flip angle = 12°*, *×220mm²*, *voxelsize = 0.8 × 0.8 × 0.8mm³*, *slice thickness 0.8 mm*, and 60 *slices*. The 3D short-time inversion recovery (3D-STIR) data were acquired using the following parameters: *SPC sequence*, *TR = 3800 ms*, *TE = 194 ms*, *FOV = 230 × 230mm²*, *voxelsize = 0.9 × 0.9 × 0.9mm³*, *slice thickness = 0.9 mm*, and 64 *slices*.

Imaging processing

In this study, we used the three methods (VBM, DBM, and SBM) based on the computational anatomy toolbox 12.8.1 (CAT12.8.1, <https://neuro-jena.github.io/cat/>), an SPM12 extension with the default pipeline. For the 3D-T1WI data, we inspected each volume for any artifact that could affect the processing, such as segmentation, normalization, and so forth.

VBM analysis

The spatial adaptive nonlocal mean filter [49] was used as the first step because noise estimation and de-noising worked the best for original (non-interpolated) data. Then, the affine-registered (to further improve the outcomes of the segmentation) was made, and the center of mass was used to roughly correct for differences in the position between the image and the template. The 3D-T1WI were segmented into different tissue types, including GM, white matter (WM), and cerebrospinal fluid (CSF). Subsequently, we used the affine registration algorithm to record all the native-space tissue segments to the standard Montreal Neurological Institute (MNI) template and resample them to $1.5 \times 1.5 \times 1.5 \text{ mm}^3$ [50, 51]. The use of the diffeomorphic anatomical registration through exponentiated algebra toolbox (DARTEL) was necessary to refine the inter-subject registration via the application of the diffeomorphic anatomical registration. The images were also modulated to preserve GM data and minimize the distortion of normalization. Finally, an 8-mm full width at half maximum (FWHM) Gaussian filter was applied to allow statistical analysis [19, 52, 53].

DBM analysis

The 3D-T1WI was converted into a DBM map for each participant using a procedure described previously [41]. The resulting nonlinear transformation from previous VBM analysis was inverted to obtain the deformation fields that mapped voxel coordinates in the subject native space (χ_1, χ_2, χ_3) to equivalent voxels in the MNI template [$u_1(\chi); u_2(\chi); u_3(\chi)$]. Then, the Jacobian matrices of the deformation were generated and estimated using the first-order approximation. The Jacobian determinant minus one ($|J| - 1$) was calculated as the voxel-wise relative deformation value to create DBM maps. This value represented the factor by which each voxel of the participant's brain expanded (positive value) or shrank (negative value) during registration to the MNI template [41] and was resampled to $1.5 \times 1.5 \times 1.5 \text{ mm}^3$ [50, 51]. Finally, an 8-mm FWHM Gaussian filter was applied to allow statistical analysis.

SBM analysis

The analysis was semi-automated by applying default parameters for all processing steps, as described by Nidzam et al. [43]. The cortical thickness was estimated using a projection-based methodology by calculating the distance between the inner (boundary between WM and GM) and outer (boundary between GM and CSF) cortical surfaces [19]. Importantly, this projection-based thickness allowed the appropriate handling of partial

volume information, sulcal blurring, and sulcal asymmetries without explicit sulcus reconstruction [54]. This step provided the topological correction for defects in the surface mesh as well as for spherical inflation and spherical registration [30, 43]. The application of an adapted DARTEL algorithm during spherical registration enabled inter-subject analysis by mapping the matrix onto a standardized spherical surface. The right and left hemispheres were then merged into a single mesh, resampled to a template space (resolution 164 k mesh) [55], and spatially smoothed. Three additional geometric cortical measures, including sulcal depth (The sulcal depth refers to the depth of the grooves or "fissures" on the surface of the brain and is thought to reflect the folding pattern of the cerebral cortex), cortical complexity [Cortical fractal dimension is a measure of the complexity of the cerebral cortex, and it can be calculated by analyzing the pattern of folding on the surface of the brain and the cortical complexity (fractal dimension) was calculated on the paper described in Yotter] [56], and gyri-fication (The gyri-fication is a measure of the complexity and folding of the cerebral cortex, which can be extracted based on the absolute mean curvature of the brain surface) [57], were also derived. A 15-mm FWHM Gaussian kernel was used for smoothing the cortical thickness images, while a 20-mm FWHM Gaussian kernel was used for other parameters as recommended [19, 43]. The smoothed images were used for between-group analyses, as described later.

TGN cisternal segment volume analysis

The 3D-VIBE or 3D-STIR images were used for the volume of the TGN cisternal segment (TGNcV) and CSA of the compression point analysis. The manual segmentation of the TGN cisternal segment from its emergence at the pons to its entry at Meckel's cave slice by slice in the axial plane and CSA of the compression point (i.e., the entire cisternal segment) was performed with the uAI Research Portal (United Imaging Intelligence, China) embedded into the widely used package PyRadiomics (<https://pyradio.mics.readthedocs.io/en/latest/index.html>) by a junior physician with 4 years of experience and a senior physician with 9 years of experience. The TGNcVs were calculated for comparison in the following ways: ipsilateral and contralateral to the side of pain in patients with CTN; the average of HCs [(right + left)/2]. The analysis of delineation consistency between the junior and senior physicians was performed using the intra-class correlation coefficient (ICC).

Statistical analysis of clinical parameters and TGN structure.

The statistical analyses of clinical variables were conducted using SPSS software (version 26). The differences

between groups were examined with independent-sample *t* tests for continuous data (age, VAS score, MMSE score, pain frequency, TGNcV, and so on) and with the chi-squared test for sex. The statistical significance was defined as $P < 0.05$.

Statistical analysis of structural images

The between-group differences in cortical thickness, sulcal depth, cortical complexity, gyri-fication (by SBM), and GMV (by DBM and VBM) were assessed with two-sample *t* tests controlling for age and sex. Total intracranial volume was also used as the covariate in the VBM models [49, 50, 58]. The two groups were compared in multiple ways: DBM and VBM based on GRF (voxels $P < 0.001$, clusters $P < 0.05$) and SBM based on family-wise error (FWE, voxels $P < 0.001$, clusters $P < 0.05$). Spearman correlations were performed on pain characteristics (disease duration, VAS, pain frequency, TN QOLS, SAS, SDS, etc.) and TGNcV for determining the correlations between mean cortical thickness/volume, gyri-fication from the clusters derived from VBM or DBM or SBM, and clinical parameters. The statistical significance was defined as $P < 0.05$, and all tests were two-tailed.

Results

Demographic information and clinical characteristics

The demographic variables and clinical characteristics of the participants are summarized in Table 1. A total of 79 patients with CTN (54F, 25 M; 54.05 ± 10.56 years old) and sex- and gender-matched 81 HCs (56F, 27F; 52.28 ± 8.56 years old) were included in this study. The inclusion process is shown in Fig. 1. All the patients with CTN had unilateral onset (52R, 27L), and the pain distribution was more in V2.3 (41/79). Most patients had severe pain intensity (VAS, 8.25 ± 1.77), and the average duration of attack was more than 2 min in 28 patients, and the peripheral or central sensitization may account for the continuous pain. Compared with HCs, patients with CTN had poorer quality of life and cognition and more severe depression and anxiety.

NVC degree and TGNcV

The ICC analysis showed that the TGNcV was in good agreement ($ICC \geq 0.75$). All the patients displayed varying degrees of NVC on the side affected. The nerve distortion and/or displacement occurred in 5 patients and the significant indentation was found in 74 patients, which was caused by compression of the offending vessel.

Compared with the contralateral TGNcV, the ipsilateral TGNcV in patients with CTN was significantly smaller ($53.90 \pm 25.75 \text{ mm}^3$ vs $68.17 \pm 30.13 \text{ mm}^3$,

Table 1 Demographic and clinical characteristics of patients with CTN and healthy controls

	CTN		HCs	P
Sex (women/men)	54/25		56/27	0.957
Age (year)	54.05 ± 10.56		52.28 ± 8.56	0.077
Lateral (R/L)	52/27		NA	NA
Distribution	V2.3	41	NA	NA
	V3	15		
	V2	13		
	V1.2	8		
	V1.2.3	1		
	V1	1		
Average duration of attack	< 2 min	51	NA	NA
	> 2 min	28		
Attack frequency (per day)	< 20	24	NA	NA
	20–50	15		
	50–100	8		
	> 100	32		
Duration (year)	5.03 ± 4.94		NA	NA
Pain intensity (VAS)	8.25 ± 1.77		NA	NA
MMSE	26.94 ± 3.20		28.54 ± 1.82	0.000
Symptoms*	21.86 ± 4.36		6.00 ± 0.00	0.000
Physical function*	19.14 ± 4.27		13.95 ± 2.36	0.000
Psychology*	13.00 ± 4.22		5.67 ± 1.26	0.000
Society*	14.29 ± 4.09		5.00 ± 0.00	0.000
Self-rating depression scale	37.38 ± 7.11		28.59 ± 5.17	0.000
Self-rating anxiety scale	33.10 ± 5.91		28.37 ± 5.35	0.000
CSA of compression point (mm ²)	11.18 ± 4.47		NA	NA
TGNcV (mm ³)	Ipsi (53.90 ± 25.75)	Contra (68.17 ± 30.13)	HCs (115.47 ± 31.59)	0.002
	Ipsi (53.90 ± 25.75)	Contra (68.17 ± 30.13)	HCs (115.47 ± 31.59)	0.000

CTN Classical trigeminal neuralgia, HCs Healthy controls; * the four dimensions of the quality-of-life score of patients with trigeminal neuralgia; R Right, L Left, MMSE Mini-mental state examination, VAS Visual analogue scale, CSA Cross-sectional area, TGNcV Volume of trigeminal nerve cisternal segment, ipsi ipsilateral, contra contralateral

$P=0.002$). Compared with the average TGNcV of the HCs, the nerves of the affected ($115.47 \pm 31.59 \text{ mm}^3$ vs $53.90 \pm 25.75 \text{ mm}^3$, $P=0.002$) or unaffected side ($115.47 \pm 31.59 \text{ mm}^3$ vs $68.17 \pm 30.13 \text{ mm}^3$, $P=0.002$) were all atrophied. The CSA of the compression point was $11.18 \pm 4.47 \text{ mm}^2$ (Table 1 and Fig. 2).

VBM analysis between CTN and HCs

The GM atrophy in patients was compared with that in HCs in two clusters: Temporal_Pole_Sup_R (10.07%) and Precentral_R (12.28%) (Fig. 3), as detected by VBM. Table 2 lists the standard space coordinates, different brain regions, and voxels of these brain regions. A positive

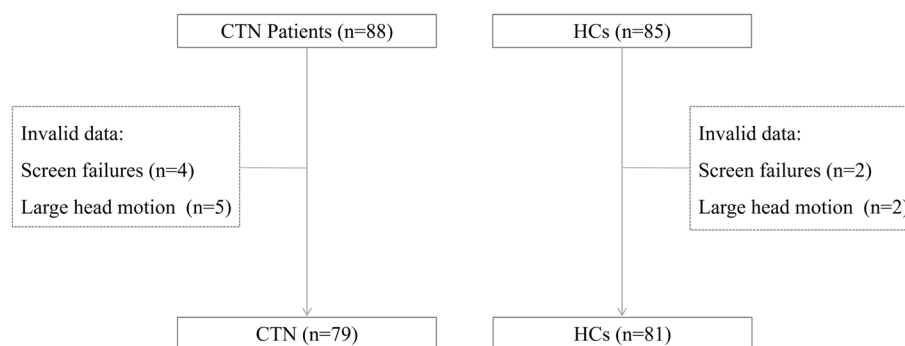


Fig. 1 Selection of patients with CTN and HCs. CTN, classical trigeminal neuralgia; HCs, healthy controls

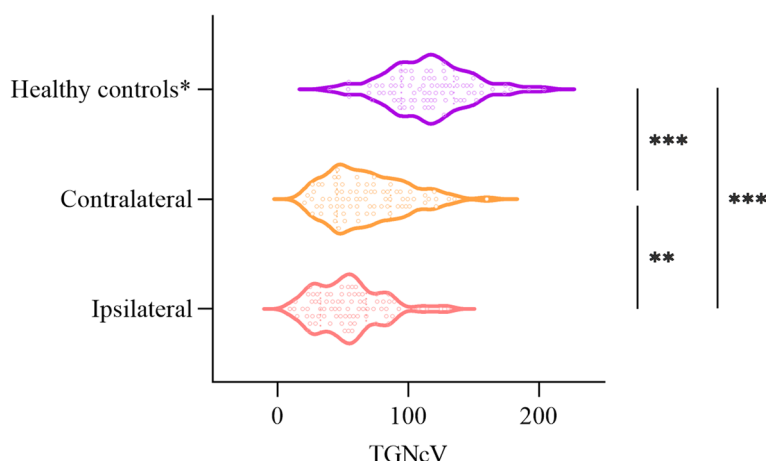


Fig. 2 The TGNCV (mm³) between patients with CTN (ipsilateral and contralateral) and healthy controls. The ipsilateral TGNCV was significantly smaller compared with the contralateral TGNCV, and the bilateral TGNCVs were both significantly smaller compared with the average TGNCV of healthy controls. *Average volume of the healthy controls ((right + left)/2); CTN, classical trigeminal neuralgia; TGNCV, volume of trigeminal nerve cisternal segment

correlation was found between the GMV of Temporal_Pole_Sup_R and disease duration (year) ($P=0.030$, $r=0.245$). A negative correlation was found between the GMV of Temporal_Pole_Sup_R and CSA of the compression point ($P=0.048$, $r=-0.224$) and symptoms of TN QOLS ($P=0.002$, $r=-0.336$). A negative correlation was found between the GMV of precentral_R and ipsilateral TGNCV ($P=0.013$, $r=-0.278$), CSA ($P=0.041$, $r=-0.231$), and VAS ($P<0.025$, $r=-0.252$) (Fig. 4).

DBM analysis between CTN and HCs

The GM volume increased in patients compared with HCs in one cluster named Temporal_Pole_Sup_L (8.16%), as detected by DBM (Fig. 3). Table 2 lists the standard space coordinates, different brain regions, and voxels of these brain regions. A negative correlation was found between the GMV of Temporal_Pole_Sup_L and SAS ($P=0.005$, $r=-0.341$) (Fig. 4).

SBM analysis between CTN and HCs

The SBM analysis across the whole brain found that the gyrification increased in the Middle Temporal_L (3.70%) and the thickness of the cortex decreased in Postcentral_L (4.92%) of patients with CTN compared with HCs (Fig. 5).

Discussion

This study involved a single-center, prospective assessment of 79 patients with CTN. The results showed that the brain regions detected by VBM, DBM, and SBM were different and complemented each other. Among these, some brain regions were correlated with the clinical parameters, TGNCV, and CSA of the compression point.

The three methods (VBM, DBM, and SBM) analyzed the change in brain neuroanatomy [42]. Among these, DBM and VBM were the voxel-level analysis methods [34, 59], which were used to measure the GMV [42]. VBM provided voxel-wise volume estimations of segmented GM, WM, and CSF [33, 37]. DBM relied on the deformation generated from the spatial registration to reflect the whole-brain structural changes [35, 60]. SBM analyzed the cortical morphological features based on vertex measurement and comparison of the cortical thickness [42]. These three brain structure analysis methods could extract different indicators, representing different structural characteristics of the brain cortex.

In this study, the GMV of Temporal_Pole_Sup_L was found to be decreased using VBM and increased using DBM. The Temporal_Pole_Sup plays an important role in pain memory, and the pain memory plays a crucial role in the perception of future pain [61, 62], indicating that

(See figure on next page.)

Fig. 3 VBM and DBM analysis of the GMV. (A) VBM analysis revealed significantly decreased GMV in two clusters in patients with CTN compared with healthy controls. GMV atrophy was observed in the Temporal_Pole_Sup_R and Precentral_R (GFR, voxels $P<0.001$, clusters $P<0.05$). (B) DBM analysis revealed significantly increased GMV cluster (Temporal_Pole_Sup_L) in patients with CTN compared with healthy controls (GFR, voxels $P<0.001$, clusters $P<0.05$). CTN, classical trigeminal neuralgia; VBM, voxel-based morphometry; DBM, deformation-based morphometry; GMV: gray matter volume; GRF: Gaussian random field

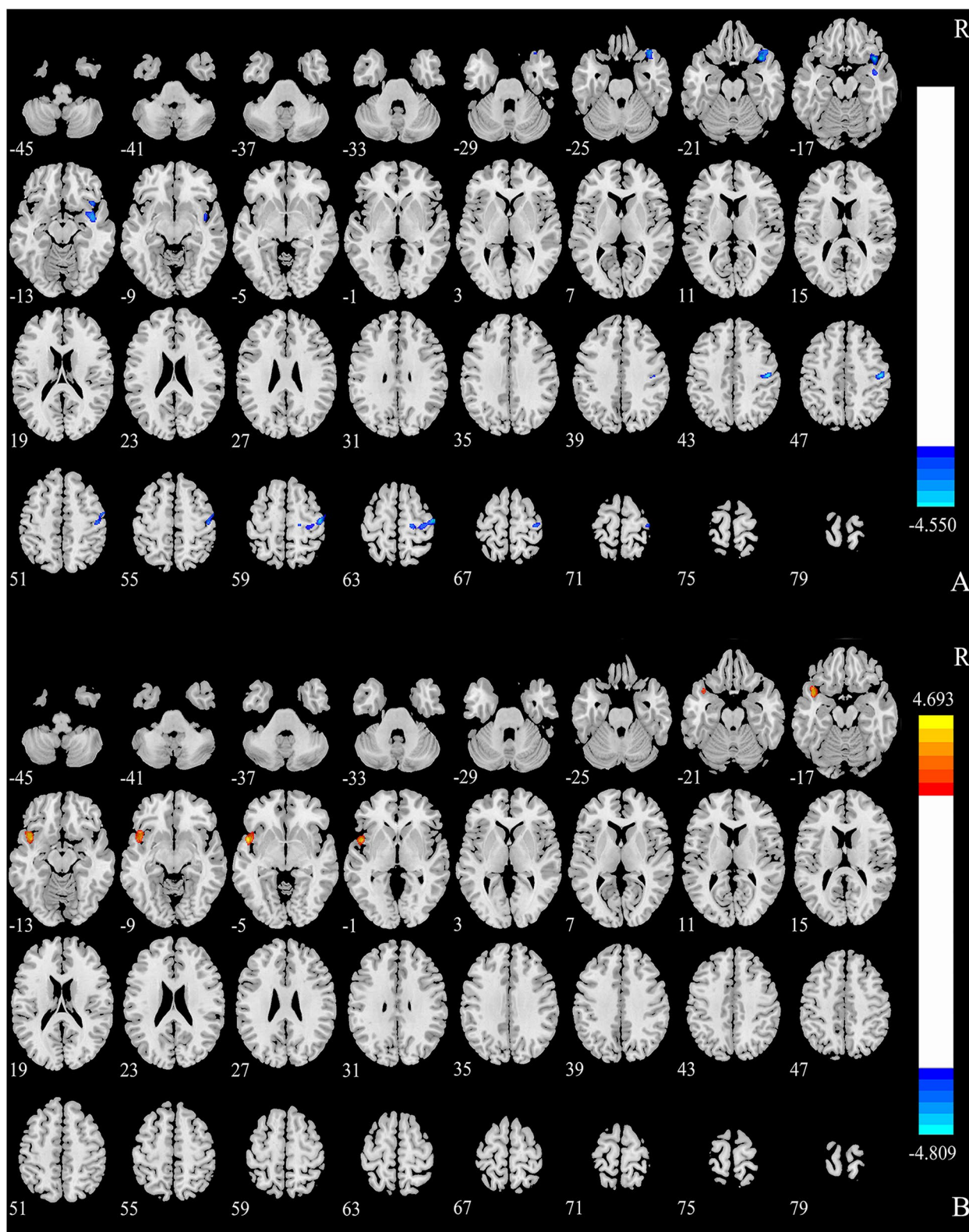


Fig. 3 (See legend on previous page.)

Table 2 Brain regions in which the GMV or cortex shape changed in patients compared with healthy controls, as detected using VBM, DBM, and SBM

	Brain region	Side	Peak MNI coordinates			Cluster size (voxels)	Peak intensity
			X	Y	Z		
VBM	TPOsup	R	39	16.5	-18	787	-4.5498
	Precentral	R	48	-16.5	45	940	-4.5072
DBM	TPOsup	L	-51	7.5	-3	762	4.6929
SBM							
Gyrification	Middle temporal gyrus	L	-39.5	-0.58	-52.1	1523	4.1882
Thickness	Postcentral	L	-38.9	13.9	13.9	1802	-3.9562

GMV Gray matter volume, CTN Classical trigeminal neuralgia, MNI Montreal Neurological Institute, VBM Voxel-based morphometry, DBM Deformation-based morphometry, SBM Surface-based morphometry, TPOsup Temporal_Pole_Sup

the Temporal_Pole_Sup might be related to pain memory in patients with CTN. The GMV and side of Temporal_Pole_Sup were different between VBM and DBM due to two reasons. On the one hand, it might be some differences between the two methods. VBM converted images into standard space for information extraction, whereas the DBM method extracted information from deformation field. Therefore, it was seen that the two methods complemented each other. On the other hand, it might be the compensatory mechanism. CTN caused a decrease in the GMV of Temporal_Pole_Sup on the right side and an increase in the compensatory volume of Temporal_Pole_Sup on the left side. Pain is a subjective experience that can produce symptoms beyond the perception of pain itself [63]. Therefore, the reason for this phenomenon may also be caused by other factors, which needs further study. Wang et al. [17] found that the GMV of bilateral Temporal_Pole_Sup decreased. Li et al. [23]

also found that the GMV of bilateral Temporal_Pole_Sup decreased and was negatively correlated with the course of disease. The previous studies on the GMV in patients with CTN mostly used VBM. Our study combined DBM and VBM to study the GMV in patients with CTN, which had a certain complementary effect on previous findings. The Temporal_Pole_Sup was also involved in emotion regulation and had neurocognitive functions [64]. The correlation analysis showed that the volume of Temporal_Pole_Sup_L decreased with the increase in anxiety. The CSA of the compression point and TN QOLS (symptoms dimension) decreased and the Temporal_Pole_Sup_R volume increased with the increase in disease duration. This indicated that the disease duration, CSA of compression point, TN QOLS (symptoms dimension), and mood might affect the Temporal_Pole_Sup GMV of patients with CTN.

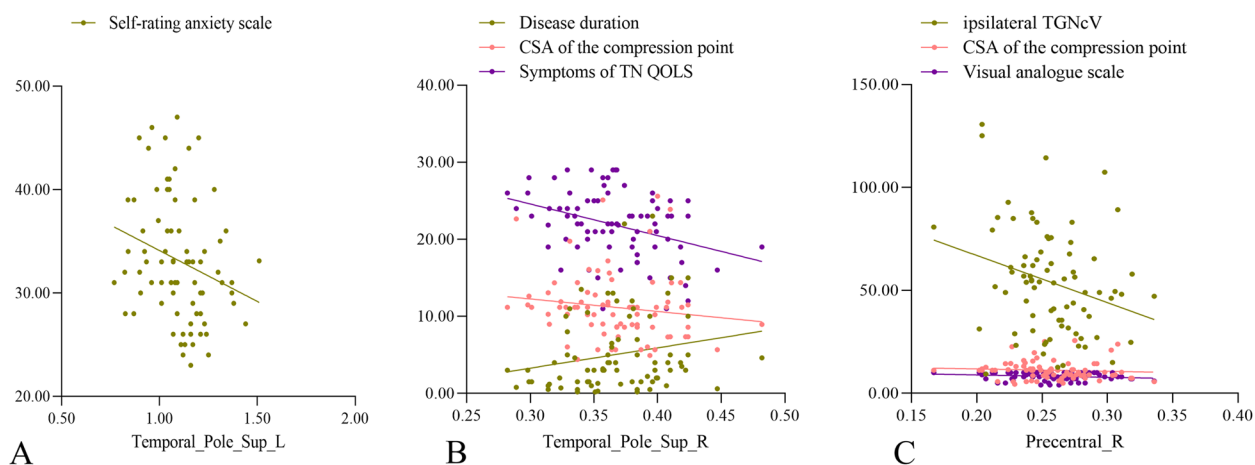


Fig. 4 Correlations between the clinical parameters and brain regions in which the GMV changed in patients with CTN. (A) The GMV of TPOsup_L was negatively correlated with self-rating anxiety scale ($P=0.005$, $r=-0.341$), (B) The GMV of TPOsup_R was positively correlated with disease duration (years) ($P=0.030$, $r=0.245$) and negatively correlated with the CSA of compression point ($P=0.048$, $r=-0.224$) and symptoms of TN QOLS ($P=0.002$, $r=-0.336$). (C) The GMV of precentral_R was negatively correlated with the ipsilateral TGnCV ($P=0.013$, $r=-0.278$), CSA of the compression point ($P=0.041$, $r=-0.231$), and VAS ($P<0.025$, $r=-0.252$). GMV, gray matter volume; CTN, classical trigeminal neuralgia; CSA, cross-sectional area; TN QOLS, quality-of-life score of patients with trigeminal neuralgia; TGnCV, volume of trigeminal nerve cisternal segment

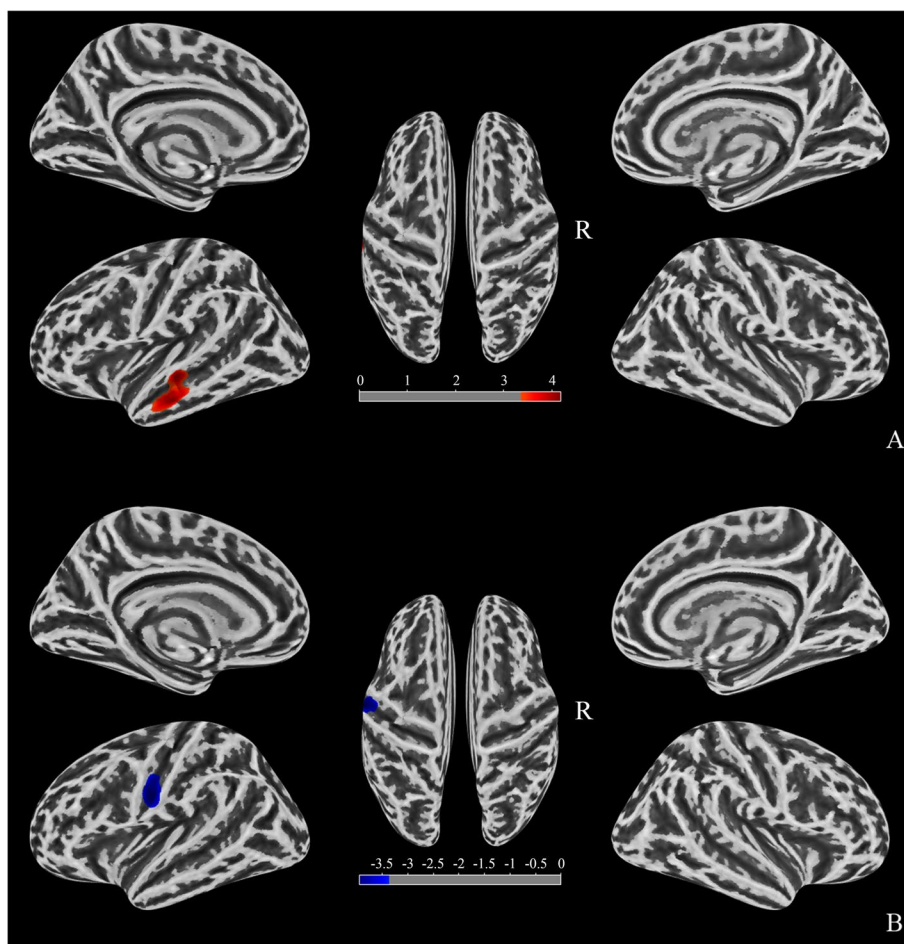


Fig. 5 A comparison of the cortical morphology of patients with CTN and healthy controls using SBM. **(A)** Gyrfication: red clusters representing significantly more gyrfication (left middle temporal gyrus) in patients with CTN (FWE, voxels $P < 0.001$, clusters $P < 0.05$). **(B)** Cortical thickness: blue clusters representing significantly thinner cortical regions (left postcentral) in patients with CTN (FWE, voxels $P < 0.001$, clusters $P < 0.05$). CTN, classical trigeminal neuralgia; SBM, surface-based morphometry; FWE, family-wise error

In this study, besides the decrease in the GMV of Temporal_Pole_Sup_R, we also found a decrease in the GMV of precentral_R using VBM. The precentral_R is located in the frontal lobe and is the main motor area of the cerebral cortex. It is a key driver of motor output and associated with pain perception and regulation [12]. CTN is often triggered by harmless movements such as washing face and eating. Patients may limit the occurrence of such movements to avoid pain, which may lead to a change in precentral GMV. Thus, the precentral_R may reflect a sensory pain response caused by repeated CTN, motor inhibition of the maxilla, and facial muscle tone [65–67]. Tsai et al. [12] and Yan et al. [68] found that the GMV decreased in precentral_R. Wang et al. [20] found that the GMV decreased in multiple brain areas, including primary motor cortex and premotor area. The correlation analysis showed that the ipsilateral TGNcV and CSA of the compression point increased, and the pain degree of patients with CTN was more severe (VAS score

was higher) with the decrease in the GMV of precentral_R. The indicated that the VAS score, ipsilateral TGNcV, and CSA of the compression point affected the GMV of precentral_R GMV.

In this study, we analyzed four parameters using SBM: sulcal depth, curvature, cortical thickness, and degree of gyrfication. Among these, we found brain regions with different degree of gyrfication and cortical thickness, while the remaining parameters displayed no changes. The middle temporal gyrus is the classic brain region of the default mode network. In this study, the gyrfication of middle temporal_L increased. This was probably because the long-term pain stimulation led to a change in the morphology of the middle temporal gyrus (gyrfication). Current studies on the brain structure of patients with TN only found a decrease in the GMV of the middle temporal gyrus. Li et al. [23] and Wang et al. [17] found that the GMV increased in the middle temporal gyrus, while Yan

et al. [68] found that the GMV decreased in the middle temporal gyrus. No study showed a change in gyrification in the middle temporal gyrus, which might be caused by individual differences and different processing methods. The postcentral is the primary somatosensory cortex, which receives most somatosensory information from the thalamus and is involved in the anticipation, intensity, discrimination, spatial and temporal summation of pain processing, and pain coding [69]. In our study, we found a decrease in the cortical thickness of Postcentra_L. Desouza et al. [32] and Obermann et al. [21] found that the thickness of the left primary sensory cortex increased in patients with TN compared with HCs.

The ultrastructural features of neurons and other cells in the cortex may contribute to the morphological characteristics that are observed at a macroscopic level [70–72]. The cortical morphology characteristics, including GMV, cortical thickness, gyrification index, and sulcal depth have been indicated to reflect the regulation of intermediate progenitor cells' genesis and amplification [30, 70]. The gray matter density, cortical area, channel pattern and cortical thickness affected the size of GMV [71]. Various cellular-level features including density, size, arrangement of neurons, nerve fibers, and neuroglia affected the cortical thickness [72]. Cortical gyrification adapts the cortical surface area to the skull, which promotes the development of neural circuits [73]. However, the exact relationship between ultrastructure and cortical morphological characteristics remains an active area of investigation, and more research is needed to fully understand this relationship.

Conclusions

In this study, we analyzed the brain structure of patients with CTN by combining VBM, DBM, and SBM. We found that some brain regions in these patients correlated with clinical parameters, TGNcV, and CSA of the compression point. However, no overlapping brain regions were found among the three methods. This might be because the processing procedures of the three methods were different, which also indicated that the three methods complemented each other. The analysis of CTN using the combination of the three methods could provide additional information and a basis for further investigation of the pathophysiology of CTN.

Limitations

In this study, the features of the recruited patients, for example, disease duration, pain distribution, pain intensity and so on, were not consistent. However, we could not perform a subgroup analysis due to sample size limitations. The sample size should be further expanded for stratified group research in the future. The other

limitation was that our study was a cross-sectional study and the longitudinal data were not included, although this was a general characteristic of most studies. Further studies should be combined with the longitudinal data to further clarify the pathophysiological mechanism of CTN.

Abbreviations

CTN	Classical trigeminal neuralgia
ICHD-3	The third edition of the International Classification of Headache Disorders
NVC	Neurovascular compression
TGN	Trigeminal nerve
TN	Trigeminal neuralgia
CSA	Cross-sectional area
HCS	Healthy controls
GMV	Gray matter volume
LGI	Local gyrification index
VBM	Voxel-based morphometry
GM	Gray matter
DBM	Deformation-based morphometry
SBM	Surface-based morphometry
VAS	Visual analogue scale
MRI	Magnetic resonance imaging
TN QOLS	Quality-of-life score of patients with TN
MMSE	Mini-mental state examination
SDS	Self-rating depression scale
SAS	Te self-rating anxiety scale
TR	Repetition time
TE	Echo time
3D-VIBE	3D volume interpolation body part examination
3D-STIR	3D short-time inversion recovery
GRF	Gaussian random fields
WM	White matter
CSF	Cerebrospinal fluid
MNI	Montreal Neurological Institute
FWHM	Full width at half maximum
FWE	Family-wise error
TGNcV	The volume of the TGN cisternal segment

Authors' contributions

XHG: data acquisition and analysis and drafting and writing of the manuscript; LYW: data analysis and important revisions to the manuscript; LP, HQY, QF, and XFZ: data collection; CF: language editing and revisions to the manuscript; QD, WHY, and ZXD: work concept or design and important revisions to the manuscript. The author(s) read and approved the final manuscript.

Funding

This study was supported by the National Natural Science Foundation of China (81871337), the Zhejiang Provincial Public Welfare Research Project (2020RC092 and 2021RC108), the Medical and Health Technology Project of Hangzhou (A20200507), and the Hangzhou Agriculture and Social Development Scientific Research Guidance Project (20211231Y022).

Declarations

Ethics approval and consent to participate

This prospective study was approved by the local ethics committee of the Hangzhou First People's Hospital, Zhejiang University School of Medicine (IRB# NO.202107002). All the participants provided written informed consent.

Competing interests

The authors declare no competing interests.

Received: 7 January 2023 Accepted: 2 February 2023
Published online: 21 February 2023

References

- Maarbjerg S, Benoliel R (2021) The changing face of trigeminal neuralgia-A narrative review. *Headache* 61(6):817–837. <https://doi.org/10.1111/head.14144>. PMID: 34214179
- DeSouza DD, Davis KD, Hodaie M (2015) Reversal of insular and micro-structural nerve abnormalities following effective surgical treatment for trigeminal neuralgia. *Pain* 156(6):1112–1123. <https://doi.org/10.1097/j.pain.000000000000156>. PMID: 25782366
- Terrier LM, Hadjikhani N, Destrieux C (2022) The trigeminal pathways. *J Neurol* 269(7):3443–3460. <https://doi.org/10.1007/s00415-022-11002-4>. Epub 2022 Mar 6 PMID: 35249132
- Cruccu G, Di Stefano G, Truini A (2020) Trigeminal Neuralgia. *N Engl J Med* 383(8):754–762. <https://doi.org/10.1056/NEJMra1914484>. PMID: 32813951
- Bendtsen L, Zakrzewska JM, Heinskou TB, Hodaie M, Leal PRL, Nurmikko T, Obermann M, Cruccu G, Maarbjerg S (2020) Advances in diagnosis, classification, pathophysiology, and management of trigeminal neuralgia. *Lancet Neurol* 19(9):784–796. [https://doi.org/10.1016/S1474-4422\(20\)30233-7](https://doi.org/10.1016/S1474-4422(20)30233-7). PMID: 32822636
- Headache Classification Committee of the International Headache Society (IHS) The International Classification of Headache Disorders, 3rd edition. *Cephalalgia*. 2018 ;38(1):1–211 <https://doi.org/10.1177/0333102417738202>. PMID: 29368949.
- Maarbjerg S, Gozalov A, Olesen J, Bendtsen L (2014) Concomitant persistent pain in classical trigeminal neuralgia—evidence for different subtypes. *Headache* 54(7):1173–83. <https://doi.org/10.1111/head.12384>. PMID: 24842632
- De Stefano G, Leone C, Di Pietro G, Esposito N, Falco P, Galosi E, Litewczuk D, Mollica C, Truini A, Di Stefano G (2022) Unravelling the role of unmyelinated nerve fibres in trigeminal neuralgia with concomitant continuous pain. *Clin Neurophysiol* 142:52–58. <https://doi.org/10.1016/j.clinph.2022.07.502>. Epub 2022 Aug 5 PMID: 35970059
- Cruccu G, Finnerup NB, Jensen TS, Scholz J, Sindou M, Svensson P, Treede RD, Zakrzewska JM, Nurmikko T (2016) Trigeminal neuralgia: New classification and diagnostic grading for practice and research. *Neurology* 87(2):220–8. <https://doi.org/10.1212/WNL.0000000000002840>. Epub 2016 Jun 15. PMID: 27306631; PMID: PMC4940067
- Maarbjerg S, Wolfram F, Gozalov A, Olesen J, Bendtsen L (2015) Significance of neurovascular contact in classical trigeminal neuralgia. *Brain* 138(Pt 2):311–319. <https://doi.org/10.1093/brain/awu349>. Epub 2014 Dec 24 PMID: 25541189
- Shankar Kikkeri N, Nagalli S. Trigeminal Neuralgia. 2022. In: StatPearls [Internet]. Treasure Island (FL): StatPearls Publishing; 2022 Jan–. PMID: 32119373.
- Tsai YH, Yuan R, Patel D, Chandrasekaran S, Weng HH, Yang JT, Lin CP, Biswal BB (2018) Altered structure and functional connection in patients with classical trigeminal neuralgia. *Hum Brain Mapp* 39(2):609–621. <https://doi.org/10.1002/hbm.23696>. Epub 2017 Nov 6. PMID: 29105886; PMID: PMC6866571
- Lee YJ, Moon HC, Tak S, Cheong C, Park YS (2019) Atrophic Changes and Diffusion Abnormalities of Affected Trigeminal Nerves in Trigeminal Neuralgia Using 7-T MRI. *Stereotact Funct Neurosurg* 97(3):169–175. <https://doi.org/10.1159/000502222>. Epub 2019 Sep 19 PMID: 31537003
- Leal PRL, Roch J, Hermier M, Berthezene Y, Sindou M (2019) Diffusion tensor imaging abnormalities of the trigeminal nerve root in patients with classical trigeminal neuralgia: a pre- and postoperative comparative study 4 years after microvascular decompression. *Acta Neurochir (Wien)* 161(7):1415–1425. <https://doi.org/10.1007/s00701-019-03913-5>. Epub 2019 May 2 PMID: 31049710
- Di Stefano G, De Stefano G, Leone C, Cruccu G, Tardioli S, Cartocci G, Fiorelli M, Truini A, Caramia F (2020) Concomitant continuous pain in patients with trigeminal neuralgia is associated with trigeminal nerve root atrophy. *Cephalalgia* 40(13):1502–1510. <https://doi.org/10.1177/0333102420949206>. Epub 2020 Aug 13 PMID: 32791919
- Alper J, Seifert AC, Verma G, Huang KH, Jacob Y, Al Qadi A, Rutland JW, Patel S, Bederson J, Shrivastava RK, Delman BN, Balchandani P (2021) Leveraging high-resolution 7-tesla MRI to derive quantitative metrics for the trigeminal nerve and subnuclei of limbic structures in trigeminal neuralgia. *J Headache Pain* 22(1):12. <https://doi.org/10.1186/s10194-021-01325-4>. PMID:34556025;PMCID:PMC8461944
- Wang Y, Yang Q, Cao D, Seminowicz D, Remeniuk B, Gao L, Zhang M (2019) Correlation between nerve atrophy, brain grey matter volume and pain severity in patients with primary trigeminal neuralgia. *Cephalalgia* 39(4):515–525. <https://doi.org/10.1177/0333102418793643>. Epub 2018 Aug 7. PMID: 30086682; PMID: PMC8889450
- Taylor KS, Anastakis DJ, Davis KD (2009) Cutting your nerve changes your brain. *Brain* 132(Pt 11):3122–3133. <https://doi.org/10.1093/brain/awp231>. Epub 2009 Sep 8 PMID: 19737843
- Wu M, Jiang X, Qiu J, Fu X, Niu C (2020) Gray and white matter abnormalities in primary trigeminal neuralgia with and without neurovascular compression. *J Headache Pain* 21(1):136. <https://doi.org/10.1186/s10194-020-01205-3>. PMID:33238886;PMCID:PMC7690170
- Wang Y, Cao DY, Remeniuk B, Krimmel S, Seminowicz DA, Zhang M (2017) Altered brain structure and function associated with sensory and affective components of classic trigeminal neuralgia. *Pain* 158(8):1561–1570. <https://doi.org/10.1097/j.pain.0000000000000951>. PMID: 28520647
- Obermann M, Rodriguez-Raecke R, Naegel S, Holle D, Mueller D, Yoon MS, Theysohn N, Blex S, Diener HC, Katsarava Z (2013) Gray matter volume reduction reflects chronic pain in trigeminal neuralgia. *Neuroimage* 1(74):352–358. <https://doi.org/10.1016/j.neuroimage.2013.02.029>. Epub 2013 Feb 26 PMID: 23485849
- Zhang Y, Mao Z, Pan L, Ling Z, Liu X, Zhang J, Yu X (2018) Dysregulation of Pain- and Emotion-Related Networks in Trigeminal Neuralgia. *Front Hum Neurosci* 20(12):107. <https://doi.org/10.3389/fnhum.2018.00107>. PMID:29662445;PMCID:PMC5890150
- Li M, Yan J, Li S, Wang T, Zhan W, Wen H, Ma X, Zhang Y, Tian J, Jiang G (2017) Reduced volume of gray matter in patients with trigeminal neuralgia. *Brain Imaging Behav* 11(2):486–492. <https://doi.org/10.1007/s11682-016-9529-2>. PMID: 26899433
- Noorani A, Hung PS, Zhang JY, Sohng K, Laperriere N, Moayed M, Hodaie M (2022) Pain Relief Reverses Hippocampal Abnormalities in Trigeminal Neuralgia. *J Pain* 23(1):141–155. <https://doi.org/10.1016/j.jpain.2021.07.004>. Epub 2021 Aug 8 PMID: 34380093
- Vaculik MF, Noorani A, Hung PS, Hodaie M (2019) Selective hippocampal subfield volume reductions in classic trigeminal neuralgia. *Neuroimage Clin* 23:101911. <https://doi.org/10.1016/j.nicl.2019.101911>. Epub 2019 Jun 26. PMID: 31491821; PMID: PMC6616529
- Albano L, Agosta F, Basaia S, Castellano A, Messina R, Parisi V, Barzaghi LR, Falini A, Mortini P, Filippi M (2022) Alterations of brain structural MRI are associated with outcome of surgical treatment in trigeminal neuralgia. *Eur J Neurol* 29(1):305–317. <https://doi.org/10.1111/ene.15105>. Epub 2021 Sep 24 PMID: 34519132
- Danylyuk H, Lee EK, Wong S, Sajida S, Broad R, Wheatley M, Elliott C, Sankar T (2020) Hippocampal and trigeminal nerve volume predict outcome of surgical treatment for trigeminal neuralgia. *Cephalalgia* 40(6):586–596. <https://doi.org/10.1177/0333102419877659>. Epub 2019 Nov 21 PMID: 31752520
- Wang Y, Zhang Y, Zhang J, Wang J, Xu J, Li J, Cui G, Zhang J (2018) Structural and functional abnormalities of the insular cortex in trigeminal neuralgia: a multimodal magnetic resonance imaging analysis. *Pain* 159(3):507–514. <https://doi.org/10.1097/j.pain.0000000000001120>. PMID: 29200179
- Moon HC, Park CA, Jeon YJ, You ST, Baek HM, Lee YJ, Cho CB, Cheong CJ, Park YS (2018) 7 Tesla magnetic resonance imaging of caudal anterior cingulate and posterior cingulate cortex atrophy in patients with trigeminal neuralgia. *Magn Reson Imaging* 51:144–150. <https://doi.org/10.1016/j.mri.2018.05.005>. Epub 2018 May 16 PMID: 29777819
- Li M, Yan J, Wen H, Lin J, Liang L, Li S, Xie S, Li W, Lin C, Jiang G (2021) Cortical thickness, gyrification and sulcal depth in trigeminal neuralgia. *Sci Rep* 11(1):16322. <https://doi.org/10.1038/s41598-021-95811-z>. PMID:34381144;PMCID:PMC8357824
- Mo J, Zhang J, Hu W, Luo F, Zhang K (2021) Whole-brain morphological alterations associated with trigeminal neuralgia. *J Headache Pain* 22(1):95. <https://doi.org/10.1186/s10194-021-01308-5>. PMID:34388960;PMCID:PMC8362283
- Desouza DD, Moayed M, Chen DQ, Davis KD, Hodaie M (2013) Sensorimotor and Pain Modulation Brain Abnormalities in Trigeminal Neuralgia:

- A Paroxysmal, Sensory-Triggered Neuropathic Pain. *PLoS One* 8(6):e66340. <https://doi.org/10.1371/journal.pone.0066340>. PMID: 23823184; PMCID: PMC3688879
33. Garrido L, Furl N, Draganski B, Weiskopf N, Stevens J, Tan GC, Driver J, Dolan RJ, Duchaine B (2009) Voxel-based morphometry reveals reduced grey matter volume in the temporal cortex of developmental prosopagnosics. *Brain* 132(Pt 12):3443–3455. <https://doi.org/10.1093/brain/awp271>. PMID:19887506;PMCID:PMC2792372
 34. Teipel SJ, Meindl T, Grinberg L, Heinsen H, Hampel H (2008) Novel MRI techniques in the assessment of dementia. *Eur J Nucl Med Mol Imaging* 35(Suppl 1):S58–69. <https://doi.org/10.1007/s00259-007-0703-z>. PMID: 18205002
 35. Ashburner J, Hutton C, Frackowiak R, Johnsrude I, Price C, Friston K (1998) Identifying global anatomical differences: deformation-based morphometry. *Hum Brain Mapp* 6(5–6):348–357. [https://doi.org/10.1002/\(SICI\)1097-0193\(1998\)6:5<693::AID-HBM4%3e3.0.CO;2-P](https://doi.org/10.1002/(SICI)1097-0193(1998)6:5<693::AID-HBM4%3e3.0.CO;2-P). PMID:9788071;PMCID:PMC6873376
 36. Honea R, Crow TJ, Passingham D, Mackay CE (2005) Regional deficits in brain volume in schizophrenia: a meta-analysis of voxel-based morphometry studies. *Am J Psychiatry* 162(12):2233–2245. <https://doi.org/10.1176/appi.ajp.162.12.2233>. PMID: 16330585
 37. Ashburner J, Friston KJ (2000) Voxel-based morphometry—the methods. *Neuroimage* 11(6 Pt 1):805–821. <https://doi.org/10.1006/nimg.2000.0582>. PMID: 10860804
 38. Borghammer J, Østergaard K, Cumming P, Gjedde A, Rodell A, Hall N, Chakravarty MM (2010) A deformation-based morphometry study of patients with early-stage Parkinson's disease. *Eur J Neurol* 17(2):314–320. <https://doi.org/10.1111/j.1468-1331.2009.02807.x>. Epub 2009 Nov 11 PMID: 19912319
 39. Scanlon C, Mueller SG, Tosun D, Cheong I, Garcia P, Barakos J, Weiner MW, Laxer KD (2011) Impact of methodologic choice for automatic detection of different aspects of brain atrophy by using temporal lobe epilepsy as a model. *AJNR Am J Neuroradiol* 32(9):1669–76. <https://doi.org/10.3174/ajnr.A2578>. Epub 2011 Aug 18. PMID: 21852375; PMCID: PMC3845529
 40. Hampel H, Bürger K, Teipel SJ, Bokde AL, Zetterberg H, Blennow K (2008) Core candidate neurochemical and imaging biomarkers of Alzheimer's disease. *Alzheimers Dement* 4(1):38–48. <https://doi.org/10.1016/j.jalz.2007.08.006>. Epub 2007 Dec 21 PMID: 18631949
 41. Tremblay C, Abbasi N, Zeighami Y, Yau Y, Dadar M, Rahayel S, Dagher A (2020) Sex effects on brain structure in de novo Parkinson's disease: a multimodal neuroimaging study. *Brain* 143(10):3052–3066. <https://doi.org/10.1093/brain/awaa234>. PMID: 32980872
 42. Ma Z, Jing B, Li Y, Yan H, Li Z, Ma X, Zhuo Z, Wei L, Li H (2020) Alzheimer's Disease Neuroimaging Initiative Identifying Mild Cognitive Impairment with Random Forest by Integrating Multiple MRI Morphological Metrics. *J Alzheimers Dis* 73(3):991–1002. <https://doi.org/10.3233/JAD-190715>. PMID: 31884464
 43. Lai KL, Niddam DM, Fuh JL, Chen WT, Wu JC, Wang SJ (2020) Cortical morphological changes in chronic migraine in a Taiwanese cohort: Surface- and voxel-based analyses. *Cephalalgia* 40(6):575–585. <https://doi.org/10.1177/0333102420920005>. Epub 2020 Apr 16 PMID: 32299230
 44. Liu X, Kakeda S, Watanabe K, Yoshimura R, Abe O, Ide S, Hayashi K, Katsuki A, Umeno-Nakano W, Watanabe R, Ueda I, Moriya J, Nakamura J, Korogi Y (2015) Relationship Between The Cortical Thickness And Serum Cortisol Levels In Drug-Naive, First-Episode Patients With Major Depressive Disorder: A Surface-Based Morphometric Study. *Depress Anxiety* 32(9):702–708. <https://doi.org/10.1002/da.22401>. Epub 2015 Aug 20 PMID: 26290363
 45. Rahayel S, Gaubert M, Postuma RB, Montplaisir J, Carrier J, Monchi O, Rémillard-Pelchat D, Bourgouin PA, Panisset M, Chouinard S, Joubert S, Gagnon JF (2019) Brain atrophy in Parkinson's disease with polysomnography-confirmed REM sleep behavior disorder. *Sleep* 42(6):zsz062. <https://doi.org/10.1093/sleep/zsz062>. PMID: 30854555; PMCID: PMC6559168
 46. Bailey JA, Zatorre RJ, Penhune VB (2014) Early musical training is linked to gray matter structure in the ventral premotor cortex and auditory-motor rhythm synchronization performance. *J Cogn Neurosci* 26(4):755–767. https://doi.org/10.1162/jocn_a_00527. Epub 2013 Nov 18 PMID: 24236696
 47. Arachchige PRW, Karunarathna S, Wataru U, Ryo U, Median AC, Yao DP, Abo M, Senoo A (2021) Changes in brain morphometry after motor rehabilitation in chronic stroke. *Somatosens Mot Res* 38(4):277–286. <https://doi.org/10.1080/08990220.2021.1968369>. Epub 2021 Sep 2 PMID: 34472386
 48. Luo Y, He M, Li C, Yang H (2019) A research on quality of life score (QOLS) of patients with trigeminal neuralgia (TN). *J Infect Public Health* 12(5):690–694. <https://doi.org/10.1016/j.jiph.2019.03.011>. Epub 2019 May 14. PMID: 31101490
 49. Manjón JV, Coupé P, Buades A, Fonov V, Louis Collins D, Robles M (2010) Non-local MRI upsampling. *Med Image Anal* 14(6):784–792. <https://doi.org/10.1016/j.media.2010.05.010>. Epub 2010 Jun 4 PMID: 20566298
 50. Neves Mde C, Albuquerque MR, Malloy-Diniz L, Nicolato R, Silva Neves F, de Souza-Duran FL, Busatto G, Corrêa H (2015) A voxel-based morphometry study of gray matter correlates of facial emotion recognition in bipolar disorder. *Psychiatry Res* 233(2):158–164. <https://doi.org/10.1016/j.pscychresns.2015.05.009>. Epub 2015 May 27 PMID: 26123449
 51. Park SE, Jeong GW (2015) Cerebral white matter volume changes in patients with obsessive-compulsive disorder: Voxel-based morphometry. *Psychiatry Clin Neurosci* 69(11):717–723. <https://doi.org/10.1111/pcn.12317>. Epub 2015 Jun 26 PMID: 25966931
 52. O'Connor EE, Zeffiro TA, Lopez OL, Becker JT (2021) Differential Effects of AIDS and Chronic Human Immunodeficiency Virus Infection on Gray Matter Volume. *Clin Infect Dis* 73(7):e2303–e2310. <https://doi.org/10.1093/cid/ciaa1552>. PMID:33053187;PMCID:PMC8492157
 53. Hirabayashi N, Hata J, Furuta Y, Ohara T, Shibata M, Hirakawa Y, Yamashita F, Yoshihara K, Kitazono T, Sudo N, Ninomiya T (2022) Association Between Diabetes and Gray Matter Atrophy Patterns in a General Older Japanese Population: The Hisayama Study. *Diabetes Care* 45(6):1364–1371. <https://doi.org/10.2337/dc21-1911>. PMID: 35500069
 54. Dahnke R, Yotter RA, Gaser C (2013) Cortical thickness and central surface estimation. *Neuroimage* 15(65):336–348. <https://doi.org/10.1016/j.neuroimage.2012.09.050>. Epub 2012 Oct 3 PMID: 23041529
 55. Baima CB, Fim NC, Alves KF, Resende LAL, Fonseca RG, Betting LE (2020) Analysis of patients with obstructive sleep apnea with and without pharyngeal myopathy using brain neuroimaging. *Sleep* 43(2):zsz216. <https://doi.org/10.1093/sleep/zsz216>. PMID: 31552419
 56. Yotter RA, Nenadic I, Ziegler G, Thompson PM, Gaser C (2011) Local cortical surface complexity maps from spherical harmonic reconstructions. *Neuroimage* 56(3):961–973. <https://doi.org/10.1016/j.neuroimage.2011.02.007>. Epub 2011 Feb 17 PMID: 21315159
 57. Luders E, Thompson PM, Narr KL, Toga AW, Jancke L, Gaser C (2006) A curvature-based approach to estimate local gyrification on the cortical surface. *Neuroimage* 29(4):1224–1230. <https://doi.org/10.1016/j.neuroimage.2005.08.049>. Epub 2005 Oct 11 PMID: 16223589
 58. Fairchild G, Sully K, Passamonti L, Stagginnus M, Darekar A, Sonuga-Barke EJS, Toschi N. Neuroanatomical markers of familial risk in adolescents with conduct disorder and their unaffected relatives. *Psychol Med* 2021:1–11. <https://doi.org/10.1017/S0033291721003202>. Epub ahead of print
 59. Sivera R, Capet N, Manera V, Fabre R, Lorenzi M, Delingette H, Pennec X, Ayache N, Robert P (2020) MAPT/DSA Group. Voxel-based assessments of treatment effects on longitudinal brain changes in the Multidomain Alzheimer Preventive Trial cohort. *Neurobiol Aging* 94:50–59. <https://doi.org/10.1016/j.neurobiolaging.2019.11.020>. Epub 2020 May 29
 60. Chung MK, Worsley KJ, Paus T, Cherif C, Collins DL, Giedd JN, Rapoport JL, Evans AC (2001) A unified statistical approach to deformation-based morphometry. *Neuroimage* 14(3):595–606. <https://doi.org/10.1006/nimg.2001.0862>
 61. Houde F, Martel M, Coulombe-Lévêque A, Harvey MP, Auclair V, Mathieu D, Whittingstall K, Goffaux P, Léonard G (2020) Perturbing the activity of the superior temporal gyrus during pain encoding prevents the exaggeration of pain memories: A virtual lesion study using single-pulse transcranial magnetic stimulation. *Neurobiol Learn Mem* 169:107174. <https://doi.org/10.1016/j.nlm.2020.107174>. Epub 2020 Jan 27
 62. De Pauw R, Coppieters I, Caeyenberghs K, Kregel J, Aerts H, Lenoir D, Cagnie B (2019) Associations between brain morphology and motor performance in chronic neck pain: A whole-brain surface-based morphometry approach. *Hum Brain Mapp* 40(14):4266–4278. <https://doi.org/10.1002/hbm.24700>. Epub 2019 Jun 20
 63. Fan L, Sun YB, Sun ZK, Wang N, Luo F, Yu F, Wang JY (2018) Modulation of auditory sensory memory by chronic clinical pain and acute experimental pain: a mismatch negativity study. *Clin Rep* 8(1):15673. <https://doi.org/10.1038/s41598-018-34099-y>

64. Huang X, Zhang D, Wang P, Mao C, Miao Z, Liu C, Xu C, Yin X, Wu X (2021) Altered amygdala effective connectivity in migraine without aura: evidence from resting-state fMRI with Granger causality analysis. *J Headache Pain* 22(1):25. <https://doi.org/10.1186/s10194-021-01240-8>
65. Wang Y, Zhang X, Guan Q, Wan L, Yi Y, Liu CF (2015) Altered regional homogeneity of spontaneous brain activity in idiopathic trigeminal neuralgia. *Neuropsychiatr Dis Treat* 13(11):2659–2666. <https://doi.org/10.2147/NDT.S94877>
66. Chen Y, Xiang CQ, Liu WF, Jiang N, Zhu PW, Ye L, Li B, Lin Q, Min YL, Su T, He LC, Shao Y (2019) Application of amplitude of low-frequency fluctuation to altered spontaneous neuronal activity in classical trigeminal neuralgia patients: A resting-state functional MRI study. *Mol Med Rep* 20(2):1707–1715. <https://doi.org/10.3892/mmr.2019.10404>
67. Zhang C, Hu H, Das SK, Yang MJ, Li B, Li Y, Xu XX, Yang HF (2020) Structural and Functional Brain Abnormalities in Trigeminal Neuralgia: A Systematic Review. *J Oral Facial Pain Headache* 34(3):222–235. <https://doi.org/10.11607/ofph.2626>
68. Yan J, Li M, Wang T, Zhan W, Jiang G (2015) Structural changes in the gray matter in patients with trigeminal neuralgia: a voxel-based morphometric study. *Nan Fang Yi Ke Da Xue Xue Bao* 35(8):1180–1183. Chinese
69. Zhu PW, Chen Y, Gong YX, Jiang N, Liu WF, Su T, Ye L, Min YL, Yuan Q, He LC, Shao Y (2020) Altered brain network centrality in patients with trigeminal neuralgia: a resting-state fMRI study. *Acta Radiol* 61(1):67–75. <https://doi.org/10.1177/0284185119847678>. Epub 2019 May 14
70. Pontious A, Kowalczyk T, Englund C, Hevner RF (2008) Role of intermediate progenitor cells in cerebral cortex development. *Dev Neurosci* 30(1–3):24–32. <https://doi.org/10.1159/000109848>
71. Yadav SA-O, Karam D, Bin Riaz I, Xie HA-O, Durani U, Duma NA-O, Giridhar KV, Hieken. Yadav S, Karam D, Bin Riaz I, Xie H, Durani U, Duma N, Giridhar KV, Hieken TJ, Ziyi Li. Measuring methods of cortical gray matter volume and cortical thickness and their application. Beijing Normal University, 2010. (Chinese)
72. Wandschneider B, Hong SJ, Bernhardt BC, Fadaie F, Vollmar C, Koepp MJ, Bernasconi N, Bernasconi A (2019) Developmental MRI markers cosegregate juvenile patients with myoclonic epilepsy and their healthy siblings. *Neurology* 93(13):e1272–e1280. <https://doi.org/10.1212/WNL.00000000000008173>. Epub 2019 Aug 29
73. Bernardoni F, King JA, Geisler D, Birkenstock J, Tam FI, Weidner K, Roessner V, White T, Ehrlich S (2018) Nutritional Status Affects Cortical Folding: Lessons Learned From Anorexia Nervosa. *Biol Psychiatry* 84(9):692–701. <https://doi.org/10.1016/j.biopsych.2018.05.008>. Epub 2018 May 23

Publisher's Note

Springer Nature remains neutral with regard to jurisdictional claims in published maps and institutional affiliations.

Ready to submit your research? Choose BMC and benefit from:

- fast, convenient online submission
- thorough peer review by experienced researchers in your field
- rapid publication on acceptance
- support for research data, including large and complex data types
- gold Open Access which fosters wider collaboration and increased citations
- maximum visibility for your research: over 100M website views per year

At BMC, research is always in progress.

Learn more biomedcentral.com/submissions

